

Multiferroics and magnetoelectrics: thin films and nanostructures

This article has been downloaded from IOPscience. Please scroll down to see the full text article.

2008 J. Phys.: Condens. Matter 20 434220

(<http://iopscience.iop.org/0953-8984/20/43/434220>)

View [the table of contents for this issue](#), or go to the [journal homepage](#) for more

Download details:

IP Address: 129.252.86.83

The article was downloaded on 29/05/2010 at 16:05

Please note that [terms and conditions apply](#).

Multiferroics and magnetoelectrics: thin films and nanostructures

L W Martin, S P Crane, Y-H Chu, M B Holcomb, M Gajek,
M Huijben, C-H Yang, N Balke and R Ramesh

Department of Materials Science and Engineering, University of California, Berkeley,
CA 94720, USA,

Department of Physics, University of California, Berkeley, CA 94720, USA
and

Materials Sciences Division, Lawrence Berkeley National Laboratory, Berkeley,
CA 94720, USA

E-mail: lwmartin@lbl.gov

Received 4 March 2008, in final form 16 April 2008

Published 9 October 2008

Online at stacks.iop.org/JPhysCM/20/434220

Abstract

Multiferroic materials, or materials that simultaneously possess two or more ferroic order parameters, have returned to the forefront of materials research. Driven by the desire to achieve new functionalities—such as electrical control of ferromagnetism at room temperature—researchers have undertaken a concerted effort to identify and understand the complexities of multiferroic materials. The ability to create high quality thin film multiferroics stands as one of the single most important landmarks in this flurry of research activity. In this review we discuss the basics of multiferroics including the important order parameters and magnetoelectric coupling in materials. We then discuss in detail the growth of single phase, horizontal multilayer, and vertical heterostructure multiferroics. The review ends with a look to the future and how multiferroics can be used to create new functionalities in materials.

(Some figures in this article are in colour only in the electronic version)

Contents

- 1. Introduction
- 2. Order parameters and scarcity of multiferroics
 - 2.1. Understanding order parameters in multiferroics
- 3. Principles and prospects for magnetoelectric multiferroics
 - 3.1. Magnetoelectric fundamentals
- 4. Thin film multiferroics
 - 4.1. Single phase multiferroic thin films
 - 4.2. Horizontal multilayer heterostructures
 - 4.3. Vertical nanostructures
- 5. New functionality with multiferroics
- 6. Future directions and conclusions

[Acknowledgments](#)

[References](#)

1. Introduction

- 1 In the last 5–8 years there has been a flurry of research focused
- 2 on multiferroic and magnetoelectric materials and much atten-
- 3 tion has been given to this field of research (including special
- 4 issues like this one) [1, 2]. From the investigation of bulk sin-
- 5 gle crystals to novel characterization techniques that probe or-
- 6 der parameters, coupling, spin dynamics, and more this is truly
- 7 a diverse field, rich with experimental and theoretical complex-
- 8 ity. By definition, a single phase multiferroic [3] is a material
- 9 that simultaneously possesses two or more of the so-called ‘fer-
- 10 roic’ order parameters—ferroelectricity, ferromagnetism, and
- 11 ferroelasticity. Magnetoelectric coupling typically refers to the
- linear magnetoelectric effect or the induction of magnetization
- by an electric field or polarization by a magnetic field [4]. The
- promise of coupling between magnetic and electronic order pa-
- rameters and the potential to manipulate one through the other
- has captured the imagination of researchers worldwide. The
- ultimate goal for device functionality would be a single phase
- multiferroic with strong coupling between ferroelectric and

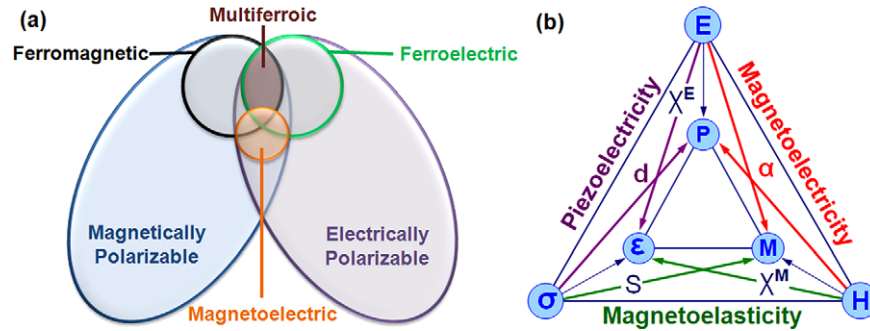


Figure 1. (a) Relationship between multiferroic and magnetoelectric materials. Illustrates the requirements to achieve both in a material (adapted from [5]). (b) Schematic illustrating different types of coupling present in materials. Much attention has been given to materials where electric and magnetic order is coupled. These materials are known as magnetoelectric materials.

ferromagnetic order parameters making for simple control over the magnetic nature of the material with an applied electric field at room temperature.

One aspect of fundamental interest to the study of multiferroics is the production of high quality samples of such materials for detailed study. In this review we will focus on the growth and characterization of thin film multiferroics (both single phase and composite) as an example of a pathway to high quality, controllable multiferroics. We will discuss the basics of and fundamental nature of order parameters in multiferroics, the coupling between order parameters in single phase and composite multiferroics, and finally the current state-of-the-art thin film multiferroic materials.

2. Order parameters and scarcity of multiferroics

2.1. Understanding order parameters in multiferroics

Multiferroism describes materials in which two or all three of the properties ferroelectricity, ferromagnetism, and ferroelasticity occur in the same phase. The overlap required of ferroic materials to be classified as multiferroic is shown schematically in figure 1(a). Only a small subgroup of all magnetically and electrically polarizable materials are either ferromagnetic or ferroelectric and fewer still simultaneously exhibit both order parameters. In these select materials, however, there is the possibility that electric fields cannot only reorient the polarization but also control magnetization; similarly, a magnetic field can change electric polarization. This functionality offers an extra degree of freedom and hence we refer to such materials as magnetolectrics (figure 1(b)). Magnetolectricity is an independent phenomenon that can arise in any material with both magnetic and electronic polarizability, regardless of whether it is multiferroic or not. By definition, a magnetolectric multiferroic must be simultaneously both ferromagnetic and ferroelectric [5]. It should be noted, however, that the current trend is to extend the definition of multiferroics to include materials possessing two or more of any of the ferroic or corresponding antiferroic properties such as antiferroelectricity and antiferromagnetism.

The scarcity of magnetolectric multiferroics can be understood by investigating a number of factors including symmetry, electronic properties, and chemistry. We note

that there are only 13 point groups that can give rise to multiferroic behavior. Additionally, ferroelectrics by definition are insulators (and in 3d transition metal based oxides, typically possess ions that have a formal d^0 electronic state), while itinerant ferromagnets need conduction electrons; even in double exchange ferromagnets such as the manganites, magnetism is mediated by incompletely filled 3d shells. Thus there exists a seeming contradiction between the conventional mechanism of off-centering in a ferroelectric and the formation of magnetic order which explains the scarcity of ferromagnetic–ferroelectric multiferroics [6]. The focus of many researchers, in turn, has been in designing and identifying new mechanisms that lead to magnetolectric coupling and multiferroic behavior. It has been proposed that one can engineer multiferroic properties by chemically controlling the functionality on a site-by-site basis. Many researchers have focused on model systems, such as the perovskites with chemical formula ABO_3 , as a pathway for the creation of multiferroic behavior. Single phase multiferroism has been identified in only a few perovskite oxides and is typically achieved by making use of the stereochemical activity of the lone pair on large (A-site) cations to provide ferroelectricity while retaining magnetism on the smaller (B-site) cations. This is the case in one of the most widely studied single phase multiferroics—the antiferromagnetic, ferroelectric $BiFeO_3$ [7]. Various alternative pathways to obtaining magnetolectric coupling are described in other review articles in this issue and we refer the reader to them for additional information [1, 8].

3. Principles and prospects for magnetolectric multiferroics

3.1. Magnetolectric fundamentals

From an applications standpoint, the real interest in multiferroic materials lies in the possibility of strong magnetolectric coupling and the possibility to create new functionalities in materials. The magnetolectric effect in its most general definition delineates the coupling between electric and magnetic fields in matter. A better understanding of magnetolectric coupling arises from expansion of the free

energy functional, i.e.

$$F(\vec{E}, \vec{H})F_0 - P_i^S E_i - M_i^S H_i - \frac{1}{2}\epsilon_0\epsilon_{ij}E_i E_j - \frac{1}{2}\mu_0\mu_{ij}H_i H_j - \frac{1}{2}\beta_{ijk}E_i H_j H_k - \frac{1}{2}\gamma_{ijk}H_i E_j E_k - \dots \quad (1)$$

with \vec{E} and \vec{H} as the electric field and magnetic field respectively. Differentiation leads to the constitutive order parameters polarization

$$P_i(\vec{E}, \vec{H}) = -\frac{\partial F}{\partial E_i} = P_i^S + \epsilon_0\epsilon_{ij}E_j + \alpha_{ij}H_j + \frac{1}{2}\beta_{ijk}H_j H_k + \gamma_{ijk}H_i E_j + \dots \quad (2)$$

and magnetization

$$M_i(\vec{E}, \vec{H}) = -\frac{\partial F}{\partial H_i} = M_i^S + \mu_0\mu_{ij}H_j + \alpha_{ij}E_i + \beta_{ijk}E_i H_j + \frac{1}{2}\gamma_{ijk}E_j E_k + \dots \quad (3)$$

where ϵ and μ are the electric and magnetic susceptibilities, respectively and α represents the induction of polarization by a magnetic field or magnetization by electric field and is known as the *linear magnetoelectric effect*. It should be noted that higher order magnetoelectric effects such as β and γ are possible, however, they are much smaller in magnitude than the lower order terms. Furthermore, the magnetoelectric response is limited by the relation $\alpha_{ij}^2 < \chi_{ii}^s \chi_{ii}^m$ where χ^s and χ^m are the electric and magnetic susceptibilities, respectively. This means that the magnetoelectric effect can only be large in ferroelectric and/or ferromagnetic materials. To date two major sources for large magnetoelectric coupling have been identified—composite materials where the magnetoelectric effect is the product property of a magnetostrictive and a piezoelectric material and multiferroic materials [4].

4. Thin film multiferroics

The re-emergence of interest in multiferroics has been driven, in part, by the development of thin film growth techniques that allow for the production of non-equilibrium phases of materials and strain engineering of existing materials [9]. Thin films offer a pathway to the discovery and stabilization of a number of new multiferroics in conjunction with the availability of high quality materials that can be produced in larger lateral sizes than single crystal samples. Multiferroic thin films and nanostructures have been produced using a wide variety of growth techniques including sputtering, spin coating, pulsed laser deposition, sol–gel processes, metal–organic chemical vapor deposition, molecular beam epitaxy, and more.

4.1. Single phase multiferroic thin films

Despite the fact that there are a number of algorithms with which one can create multiferroism in materials, to date the only single phase multiferroics produced as thin films include the hexagonal manganites and Bi- and Pb-based perovskites.

4.1.1. YMnO₃ thin films. One of the earliest thin film multiferroics to be produced was the hexagonal manganite YMnO₃ (YMO) [10]. Work on YMO in the 1960s suggested that it was both a ferroelectric [11] and an A-type antiferromagnet [12]; however, it was not until sometime later that the true nature of ferroelectricity in this material was understood to arise from long range dipole–dipole interactions and oxygen rotations working together to drive the system towards the stable ferroelectric state [13]. The first films [10] were grown via radio-frequency magnetron sputtering and obtained epitaxial (0001) films on MgO(111) and ZnO (0001)/sapphire (0001) and polycrystalline films on Pt(111)/MgO(111). It was soon shown that using the epitaxial strain intrinsic to such thin films, one could drive the hexagonal phase of YMO to a metastable, non-ferroelectric orthorhombic perovskite phase by growth on the appropriate oxide substrates including SrTiO₃(001) and NdGaO₃(101) [14]. This work was of great interest because it was the first evidence for a competition between hexagonal and orthorhombic YMO phases and how epitaxial thin film strain could be used to influence the structure of this material. This is a perfect example of the power of epitaxial thin film growth and how it can give researchers access to high pressure and temperature phases that are not easily accessible by traditional bulk synthesis techniques. Since this time YMO has been grown on a number of other substrates including Si(001) [10, 15], Pt/TiO_x/SiO₂/Si(001) [16], Y-stabilized ZrO₂(111) [17], and GaN/sapphire (0001) [18, 19] and with a wide range of deposition techniques including sputtering [15, 18], spin coating [16], sol–gel processes [20], pulsed laser deposition [21, 22], metal–organic chemical vapor deposition [23] and molecular beam epitaxy [18].

Although thin films of YMO typically exhibit a reduction in the ferroelectric polarization as compared to bulk single crystals [10], high quality epitaxial films of YMO have also been shown to possess better ferroelectric properties than oriented-polycrystalline films [24]. Polarization–electric field (P–E) hysteresis loops for YMO films have revealed that the saturation polarization in YMO is rather small (just a few $\mu\text{C cm}^{-2}$) and that films can have a retention time of 10^4 s at ± 15 V applied fields. Such results have led some to suggest that YMO films could be a suitable material for ferroelectric gate field-effect transistors [24], but the high growth temperatures (800 [24, 25]–850°C [26]) make it impractical for integration into current applications. Work has also shown that doping the A-site with more than 5%–Bi can decrease the deposition temperatures to under 700°C without detrimentally affecting the electric properties of the material [26]. Like many other manganites, however, A-site doping can also have strong effects on the properties of YMO [27]. A-site doping with Zr has been shown to decrease leakage currents, while doping with Li and Mg has been found to lead to increases in leakage currents, and finally Li-doping can also drive the antiferromagnetic YMO to become a weak ferromagnet [25]. The weak ferromagnetic moment is thought to have arisen from a small canting of the Mn spins. The hope that by controlling the carrier concentration researchers could make the normally antiferromagnetic YMO a robust

ferromagnet has not been realized. Additionally, doping on the B-site has been shown to enhance the magnetoelectric coupling in the form of changes in the magnetocapacitance by two orders of magnitude [28].

Over the last few years thin films of a wide range of hexagonal-REMnO₃ materials have been grown. This includes studies of films with RE = Nd, Ho, Tm, Lu [29], Yb [30], and more recently Tb [31], Dy, Gd, and Sm [32]. Despite all of this focus, researchers have yet to find a REMnO₃ compound that exhibits both room temperature ferroelectricity and magnetism, but hexagonal manganites remains a diverse system with intriguing scientific implications for multiferroic materials. It also serves as a model system to introduce the use of thin film growth techniques in the growth of multiferroic materials. The role of epitaxial strain in stabilizing the hexagonal-REMnO₃ phases is paramount in creating high quality samples of these materials for further study.

4.1.2. BiMnO₃ thin films. Conventional growth of bulk samples of the ferromagnetic, ferroelectric [33] BiMnO₃ (BMO) required high temperatures and pressures [34] because the phase is not normally stable at atmospheric pressure. Such phases lend themselves well to thin film growth where epitaxial strain stabilization of metastable phases can be achieved. The first growth of BMO thin films was on SrTiO₃(001) single crystal substrates using pulsed laser deposition [35] and was quickly confirmed in other studies [36]. Films of BMO have been found to be ferroelectric below ~450 K and undergo an unusual orbital ordering leading to ferromagnetism at ~105 K [37].

Temperature dependent magnetic measurements have also shown that the ferromagnetic transition temperature varies depending on the substrate and can be as low as 50 K on LaAlO₃ [38]. This depression in Curie temperature has been attributed to concepts as varied as stoichiometry issues, strain, and size effects. The ferromagnetic nature of BMO has led some to study it as a potential barrier layer in magnetically and electrically controlled tunnel junctions [39] and has eventually led to the production of a four-state memory concept based on La-doped BMO multiferroics [40]. Gajek *et al* reported La-doped BMO films that retained their multiferroic character down to thicknesses less than 2 nm and proved that multiferroic materials could be used to create new memories and opened the pathway to more study of spin-dependent tunneling using multiferroic barrier layers in magnetic tunnel junctions. More recently, significantly La-doped BMO films have been shown to exhibit a 70-fold increase in the magnetodielectric effect compared to pure BMO [41]. Unfortunately, it coincides with a decrease in the ferroelectric Curie temperature to ~150 K and is observed only at applied magnetic fields of 9 T. Additionally, optical second-harmonic measurements with applied electric fields [36], as well as Kelvin force microscopy techniques [38], have been used to confirm the presence of ferroelectric polarization in BMO films. High levels of leakage, however, have limited direct P–E hysteresis loop measurements on thin film samples and recently the reanalysis of diffraction data [42] and first principles calculations [43] have called into question the ferroelectricity in BMO. Some calculations have

predicted a small polar canting of an otherwise antiferroelectric structure (weak ferroelectricity) that could be used to explain the experimental findings [44].

4.1.3. BiFeO₃ thin films. No other single phase multiferroic has experienced the same level of attention as BiFeO₃ (BFO) in the last five years and because of this we will discuss the evolution of this material in more length. The perovskite BFO was first produced in the late 1950s [45] and many of the early studies were focused on the same concepts important today—the potential for magnetoelectric coupling [46]. Throughout the 1960s and 1970s much controversy surrounded the true physical and structural properties of BFO, but as early as the 1960s BFO was suspected to be an antiferromagnetic, ferroelectric multiferroic [47, 48]. The true ferroelectric nature of BFO, however, remained somewhat in question until ferroelectric measurements made at 77 K in 1970 [48] revealed a spontaneous polarization of ~6.1 $\mu\text{C cm}^{-2}$ along the 111-direction and were found to be consistent with the rhombohedral polar space group $R3c$ determined from single crystal x-ray diffractions (XRD) [49] and neutron diffraction studies [50]. These findings were confirmed by detailed structural characterization of ferroelectric/ferroelastic monodomain single crystal samples of BFO in the late 1980s [46]. Chemical etching experiments on ferroelastic single domains later proved without a doubt that the BFO was indeed polar and put to rest the hypothesis that BFO might be antiferroelectric and proved that the ferroelectric/ferroelastic phase was stable from 4 to ~1103 K [51]. The structure of BFO can be characterized by two distorted perovskite blocks connected along their body diagonal or the pseudocubic $\langle 111 \rangle$, to build a rhombohedral unit cell (figure 2(a)). In this structure the two oxygen octahedra of the cells connected along the $\langle 111 \rangle$ are rotated clockwise and counterclockwise around the $\langle 111 \rangle$ by $\pm 13.8^\circ$ and the Fe-ion is shifted by 0.135 Å along the same axis away from the oxygen octahedron center position. The ferroelectric state is realized by a large displacement of the Bi-ions relative to the FeO₆ octahedra (figures 2(a)–(c)) [46, 52].

During the 1980s, the magnetic nature of BFO was studied in detail. Early studies indicated that BFO was a G-type antiferromagnet (shown schematically figure 2(d)) with a Néel temperature of ~673 K [53] and possessed a cycloidal spin structure with a period of ~620 Å [54]. This spin structure was found to be incommensurate with the structural lattice and was superimposed on the antiferromagnetic order. It was also noted that if the moments were oriented perpendicular to the $\langle 111 \rangle$ -polarization direction the symmetry also permits a small canting of the moments in the structure resulting in a weak ferromagnetic moment of the Dzyaloshinskii–Moriya type (figure 4(d)) [55, 56].

In 2003 a paper focusing on the growth and properties of thin films of BFO spawned a hailstorm of research into thin films of BFO that continues to the present day. The paper reported enhancements of polarization and related properties in heteroepitaxially constrained thin films of BFO [7]. Structural analysis of the films suggested differences between films (with a monoclinic structure) and bulk single crystals

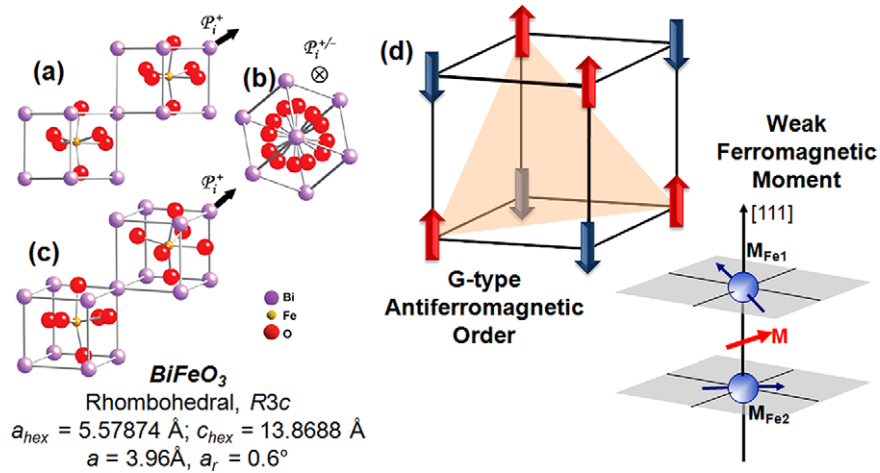


Figure 2. (a) Structure of BiFeO₃ shown looking (a) down the pseudocubic-[110], (b) down the pseudocubic-[111]-polarization direction, and (c) a general three-dimensional view of the structure. Adapted from [52]. (d) The magnetic structure of BiFeO₃ is shown including G-type antiferromagnetic ordering and the formation of the weak ferromagnetic moment.

(with a rhombohedral structure) as well as enhancement of the polarization up to $\sim 90 \mu\text{C cm}^{-2}$ at room temperature and enhanced thickness-dependent magnetism compared to bulk samples. Most importantly this report indicated a magnetoelectric coupling coefficient as high as 3 V cm Oe^{-1} at zero field [7]. A series of detailed first principles calculations utilizing the local spin-density approximation (LSDA) and LSDA + U methods helped shed light on the findings in this paper. Calculations of the spontaneous polarization in BFO suggested a value between $90\text{--}100 \mu\text{C cm}^{-2}$ (consistent with those measured in 2003) [57] and has since been confirmed by many other experimental reports. Other theoretical treatments attempted to understand the nature of magnetism and coupling between order parameters in BFO. Such calculations confirmed the possibility of weak ferromagnetism arising from a canting of the antiferromagnetic moments in BFO. The canting angle was calculated to be $\sim 1^\circ$ and would result in a small, but measurable, magnetization of $\sim 0.05 \mu_B$ per unit cell [58]. It was also found that the magnetization should be confined to an energetically degenerate easy {111} perpendicular to the polarization direction in BFO. These same calculations further discussed the connection of the weak ferromagnetism and the structure (and therefore ferroelectric nature) of BFO. This allowed the authors to extract three conditions necessary to achieve electric-field-induced magnetization reversal: (i) the rotational and polar distortions must be coupled; (ii) the degeneracy between different configurations of polarization and magnetization alignment must be broken; (iii) there must be only one easy magnetization axis in the (111) which could be easily achieved by straining the material [57].

Magnetism in thin film BFO continues to be a contentious subject to this date. The original work of Wang *et al* presented an anomalously large value of moment (of the order of 70 emu cm^{-3}) [7], which is significantly higher than the canted moment of $\sim 8 \text{ emu cm}^{-3}$. There have been several studies aimed at clarifying the origins of this anomalous magnetism. The work of Bea *et al* suggested the possibility of the formation of ferromagnetic gamma Fe₂O₃ as an impurity

phase [59]. The work of Wang *et al*, however, found no evidence (with XRD or TEM techniques) for such second phases. Furthermore, subsequent x-ray magnetic circular dichroism studies supported the assertion that this magnetism is *not* from a magnetic $\gamma\text{-Fe}_2\text{O}_3$ impurity phase. To date mixed reports, including reports of enhanced magnetism in nanoparticles of BFO [60] as well observation of samples exhibiting no such enhancement, have been presented. It is thus fair to say that as of date this issue remains unresolved in a rigorous sense.

Recent studies in our lab, however, have revealed some interesting aspects related to magnetism in epitaxial, (001)-oriented thin films of BFO. There is now a growing consensus that epitaxial films (with a thickness less than $\sim 100 \text{ nm}$) are highly strained and thus the crystal structure is more akin to a monoclinic phase rather than the bulk rhombohedral structure. Furthermore, we have observed a systematic dependence of the ferroelectric domain structure in the film as a function of the growth rate. Films grown very slowly (for example by MBE, off-axis sputtering) exhibit a classical stripe-like domain structure that is similar to ferroelastic domains in tetragonal Pb(Zr, Ti)O₃ films. Due to symmetry considerations, two sets of such twins are observed. These twins are made up of 71° ferroelastic walls, that form on the {101}-type planes (which is a symmetry plane). In contrast, if the films are grown rapidly (as was done in the original work of Wang *et al* [7]) the domain structure is dramatically different. It now resembles a mosaic-like ensemble that consists of a dense distribution of 71° , 109° , and 180° domain walls. It should be noted that 109° domain walls form on {001}-type planes (which is not a symmetry plane for this structure). Preliminary measurements reveal a systematic difference in magnetic moment between samples possessing different types and distributions of domain walls.

More recently, much has been learned about the growth, structure, and resulting properties of BFO thin films. Although many researchers anticipated strong magnetoelectric coupling in BFO, until the first evidence for this coupling in 2003 [7] there was no definitive proof. Three years

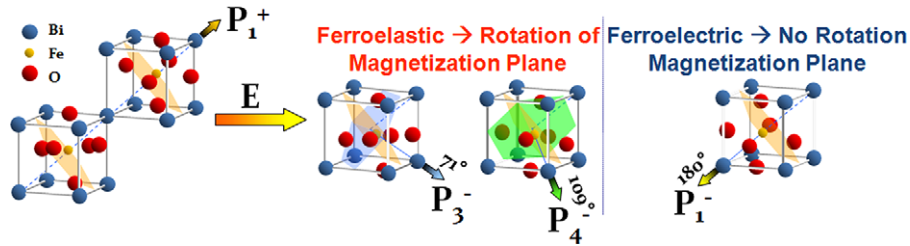


Figure 3. Schematic illustration of coupling between ferroelectricity and antiferromagnetism in BiFeO_3 . Upon electrically switching BiFeO_3 by the appropriate ferroelastic switching events (i.e., 71° and 109° changes in polarization) a corresponding change in the nature of antiferromagnetism is observed.

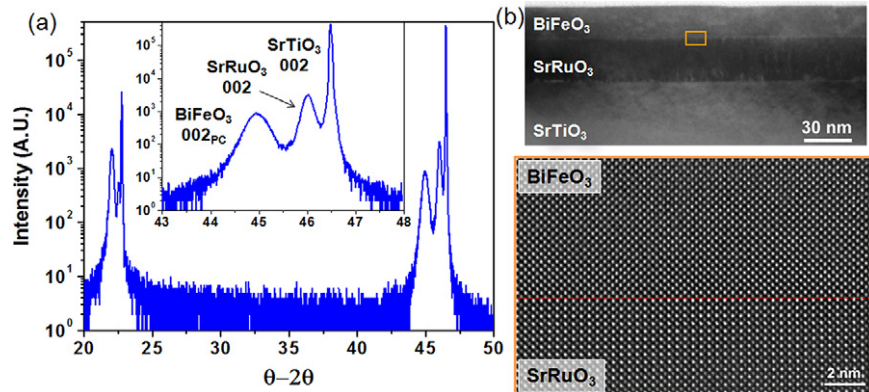


Figure 4. (a) X-ray diffraction results from a fully epitaxial, single phase BFO/SRO/STO(001) heterostructure. (b) Low and high resolution transmission electron microscopy images of BFO/SRO/STO(001) heterostructure.

after this first report, a detailed report was published in which researchers observed the first visual evidence for electrical control of antiferromagnetic domain structures in a single phase multiferroic at room temperature. By combining piezoresponse force microscopy (PFM) imaging of ferroelectric domains and x-ray photoemission electron microscopy (PEEM) imaging of antiferromagnetic domains the researchers were able to observe direct changes in the nature of the antiferromagnetic domain structure in BFO with application of an applied electric field [61]. This research showed that the ferroelastic switching events (i.e., 71° and 109°) resulted in a corresponding rotation of the magnetization plane in BFO (figure 3) and has paved the way for further study of this material in attempts to gain room temperature control of ferromagnetism (this will be discussed in detail later). This work has since been confirmed by neutron diffraction experiments in bulk BFO [62].

Today, much progress has been made in understanding the structure, properties, and growth of thin films of BFO. High quality epitaxial BFO films have been grown via pulsed laser deposition [7, 63], radio-frequency (RF) sputtering, [64, 65] metalorganic chemical vapor deposition (MOCVD) [66, 67], and chemical solution deposition (CSD) [68] on a wide range of substrates including traditional oxide substrates as well as Si [63, 69] and GaN [70]. This work has shown that high quality films, like those shown in figure 4 can be produced. Typical XRD θ - 2θ measurements (figure 4(a)) show the ability of researchers to produce high quality, fully epitaxial, single phase films of BFO (data here is for a

BFO/SrRuO₃(SRO)/SrTiO₃(001) heterostructure). Detailed XRD analysis has shown that films possess a monoclinic distortion of the bulk rhombohedral structure over a wide range of thicknesses, but the true structure of very thin films (<15 nm) remains unclear [71]. The quality of such heterostructures as produced by pulsed laser deposition can be probed further by transmission electron microscopy (TEM) (figure 4(b)). TEM imaging reveals films that are uniform over large areas and with the use of high resolution TEM we can examine the atomically abrupt, smooth, and coherent interface between BFO and a commonly used bottom electrode material SRO.

It has also been shown that a large number of variables in the growth process can be used to effect significant changes in the nature of ferroelectricity in BFO. Such control and the ability to create periodic domain structures in BFO could give rise to interesting photonic devices, new pathways for nanolithography, as well as new devices that take advantage of the multiferroic nature of BFO. Theoretical models have predicted that one could control the ferroelectric domain structure of BFO through careful control of thin film heteroepitaxial growth constraints [72]. For instance it has been shown that selection of the appropriate substrate material possessing anisotropic in-plane lattice parameters can give rise to self-oriented, 1D periodic ferroelectric domain structures in BFO films [73]. Focusing on heterostructures like those shown in figure 5(a), the authors took advantage of the close lattice matching between BFO, SRO, and DyScO₃ (DSO) (110) and the anisotropic in-plane lattice parameters of DSO

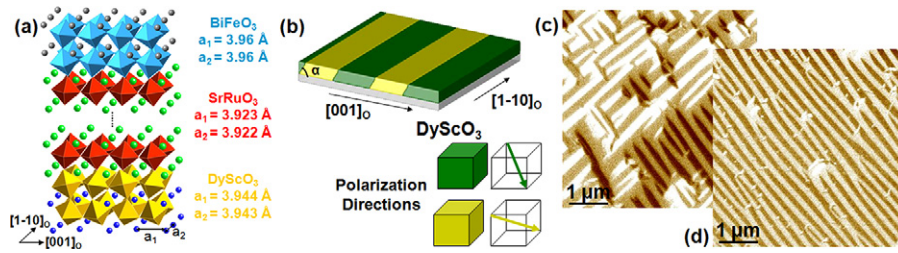


Figure 5. (a) Schematic of the BFO/SRO/DSO heterostructures and (b) domain structure of the BFO film as predicted by phase-field simulations. In-plane piezoresponse force microscopy images of the ferroelectric domain structure in BFO films showing (c) 4-polarization variants and (d) 2-polarization variants. Adapted from [73].

($a_1 = 3.951 \text{ \AA}$ and $a_2 = 3.946 \text{ \AA}$) to pin the structure of the SRO layer and, in turn, the FE domain structure of BFO. Phase-field modeling of the ferroelectric domain structure in such heterostructures (figure 5(b)) predicted stripe-like ferroelectric domain structures which were confirmed in the final BFO films (figures 5(c) and (d)). The growth mechanism of the underlying SRO layer was found to be important in determining the final ferroelectric domain structure of the BFO films. SRO layers grown via step-bunching and step-flow growth mechanisms resulted in ferroelectric domain structures with 4-polarization variants (figure 5(c)) and 2-polarization variants (figure 5(d)), respectively. These films have been shown to exhibit excellent ferroelectric properties with room temperature $2P_r \sim 120\text{--}130 \mu\text{C cm}^{-2}$ and strong intrinsic ferroelectric properties [74].

Another pathway to control domain structures in BFO is through the use of substrate orientation and vicinality. Growth of BFO thin films on STO (001), (110), and (111) substrates results in films with 4-, 2-, and 1-polarization variants because of the fundamental symmetry of the rhombohedral BFO structure [75]. Measurement of room temperature P–E hysteresis loops for BFO films grown on these substrates reveals that the measured magnitude of the saturation polarization increases as one moves from (001)- to (110)- to (111)-oriented films as the projection of the polarization axis lies closer to the direction of measurement. It was further found that with appropriate selection of vicinally-miscut STO (001) substrates, (001) films with ferroelectric domain structures possessing 4-, 2-, and 1-polarization variant can be produced as well. These examples represent the current state of the art control of domain structures in BFO thin films and, as we will investigate in the next section, have been shown to be of great interest for current studies of coupling BFO.

In the last few years, attention has also been given to studying doped BFO thin films (both A-site and B-site doping) in attempts to reduce leakage currents and alter the magnetic properties [76]. Doping the B-site of BFO with Ti^{4+} has been shown to lead to an increase in film resistivity by over three orders of magnitude while doping with Ni^{2+} has been shown to decrease resistivity by over two orders of magnitude [77]. Doping with Cr has also been shown to greatly reduce leakage currents in BFO films [78]. There are many studies focusing on doping BFO, but little significant impact on the physical properties has been achieved.

4.1.4. Other single phase multiferroic thin films. Finally, we note that a number of other candidate multiferroic materials with lone-pair active A-sites and magnetic transition metal B-sites have been produced in the last few years. Thin films of BiCrO_3 were grown on $\text{LaAlO}_3(001)$, STO (001), and $\text{NdGaO}_3(110)$ substrates and were shown to display weak ferromagnetism with a Curie temperature of $\sim 120 \text{ K}$ and evidence for piezoelectric response at room temperature [79]. Bulk work on BiCoO_3 [80] and theoretical predictions of giant electronic polarization of more than $150 \mu\text{C cm}^{-2}$ [81] have driven researchers to attempt creating this phase as a thin film as well. To date only solid solutions of $\text{BiFeO}_3\text{--BiCoO}_3$ have been grown via MOCVD [82]. Another phase similar to BiCoO_3 that has been produced as a thin film is PbVO_3 [83]. PbVO_3 films were grown on LaAlO_3 , SrTiO_3 , $(\text{La}_{0.18}\text{Sr}_{0.82})(\text{Al}_{0.59}\text{Ta}_{0.41})\text{O}_3$, NdGaO_3 , and LaAlO_3/Si substrates and were found to be a highly tetragonal perovskite phase with a c/a lattice parameter ratio of 1.32. Further analysis of this material using second-harmonic generation and x-ray dichroism measurements revealed that PbVO_3 is both a polar, piezoelectric and likely an antiferromagnet below $\sim 130 \text{ K}$ [84]. There has also been attention given to double-perovskite structures such as $\text{Bi}_2\text{NiMnO}_6$ which have been shown to be both ferromagnetic ($T_C \sim 100 \text{ K}$) and ferroelectric with spontaneous polarization of $\sim 5 \mu\text{C cm}^{-2}$ [85].

4.2. Horizontal multilayer heterostructures

Great strides have been made in the area of composite magnetoelectric systems. These systems operate by coupling the magnetic and electric properties between two materials, generally a ferroelectric material and a ferrimagnetic material, via strain. An applied electric field creates a piezoelectric strain in the ferroelectric, which produces a corresponding strain in the ferrimagnetic material and a subsequent piezomagnetic change in magnetization or the magnetic anisotropy. Work started in the field several decades ago using bulk composites, although experimental magnetoelectric voltage coefficients were far below those calculated theoretically [86]. In the 1990s theoretical calculations showed possible strong magnetoelectric coupling in a multilayer (2-2) configuration; an ideal structure of the burgeoning field of complex oxide thin film growth [87]. In this spirit, researchers experimentally tested a number of materials in a laminate thick film geometry, including ferroelectrics such as $\text{Pb}(\text{Zr}, \text{Ti})\text{O}_3$ [88–93],

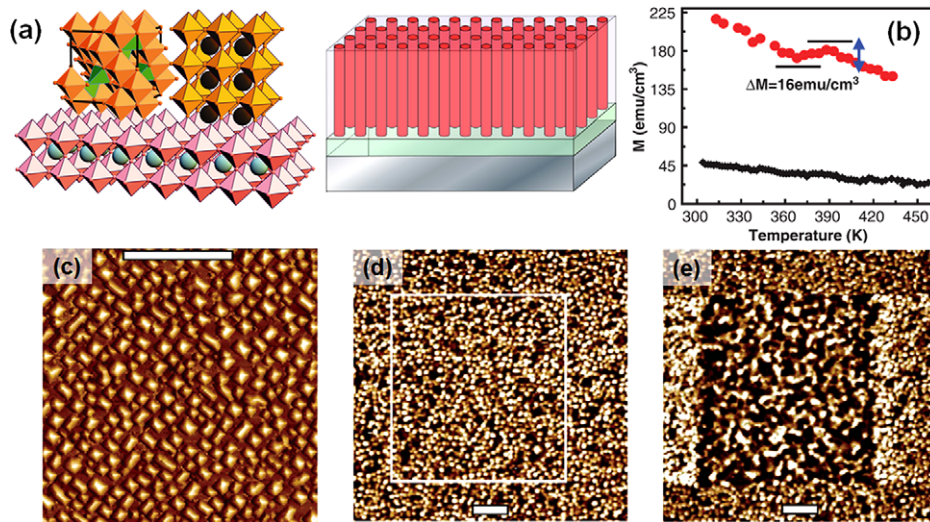


Figure 6. (a) Schematic illustrations of vertical nanostructure of spinel pillars embedded in a perovskite matrix grown on a perovskite substrate. (b) Magnetization versus temperature curve measured at 100 Oe showing a distinct drop in magnetization at the ferroelectric Curie temperature—proof of strong magnetoelectric coupling. (c) Surface topography of a $\text{CoFe}_2\text{O}_4/\text{BiFeO}_3$ nanostructure as imaged by atomic force microscopy. Magnetic force microscopy scans taken in the same area before (d) and after electrical poling at -16 V (e) (scale bars are $1 \mu\text{m}$). Adapted from [98, 108].

$\text{Pb}(\text{Mg}_{0.33}\text{Nb}_{0.67})\text{O}_3\text{-PbTiO}_3$ (PMN-PT) [94], and ferromagnets such as TbDyFe₂ (Terfenol-D) [88], NiFe₂O₄ [89, 91], CoFe₂O₄ [93], Ni_{0.8}Zn_{0.2}Fe₂O₄ [90], La_{0.7}Sr_{0.3}MnO₃ [92], La_{0.7}Ca_{0.3}MnO₃ [92]. These experiments showed promise, displaying magnetoelectric voltage coefficients up to $\Delta E/\Delta H = 4680 \text{ mV cm}^{-1} \text{ Oe}^{-1}$. Work also continued investigating thin film heterostructures by combining such ferroelectrics as Ba_{0.6}Sr_{0.4}TiO₃, BaTiO₃ [95], and PMN-PT [96] with the ferromagnet Pr_{0.85}Ca_{0.15}MnO₃ [95] and Tb-Fe/Fe-Co multilayers [96]. However, these attempts were unable to produce magnetoelectric voltage coefficients above a few tens of $\text{mV cm}^{-1} \text{ Oe}^{-1}$. Current theories suggest that the in-plane magnetoelectric interface is limiting the magnitude of this coefficient due to the clamping effect of the substrate on the ferroelectric phase [97]. Since the amount of the ferroelectric phase can strain is limited via this in-plane interfacial geometry, the magnetoelectric voltage coefficient can be reduced by up to a factor of five.

4.3. Vertical nanostructures

A seminal paper by Zheng *et al* showed that magnetoelectric materials could also be fabricated in a nanostructured columnar fashion (figure 6(a)) [98]. By selecting materials that spontaneously separate due to immiscibility, such as spinel and perovskite phases [86], one can create nanostructured phases made of pillars of one material embedded in a matrix of the other. In this initial paper, researchers reported structures consisting of CoFe₂O₄ (CFO) pillars embedded in a BaTiO₃ (BTO) matrix. The large difference in lattice parameter between these phases leads to the formation of pillars with dimensions on the order of tens of nanometers, which ensures a high interface-to-volume ratio, an important parameter when attempting to couple the two materials via strain. Such structures were shown to exhibit strong magnetoelectric coupling (figure 6(b)) via changes in magnetization occurring

at the ferroelectric Curie temperature of the matrix material. These nanostructures, in which the interface is perpendicular to the substrate, remove the effect of substrate clamping and allow for better strain-induced coupling between the two phases. An explosion of research into alternate material systems followed as the design algorithm proved to be widely applicable to many perovskite–spinel systems. Nanostructured composites with combinations of a number of perovskite (BTO [99], PbTiO₃ [100], Pb(Zr, Ti)O₃ [101, 102], and BFO [103, 104]) and spinel (CFO [101, 102], NiFe₂O₄ [100, 103], and γ -Fe₂O₃ [104]) or corundum (α -Fe₂O₃ [104]) structures have been investigated. The magnetic properties of such systems are generally well-behaved, but the ferroelectric properties are highly dependent on the synthesis technique. When satisfactory ferroelectric properties can be produced, more substantial magnetoelectric voltage coefficients are achieved. Pulsed laser deposition has proven to be a successful growth technique for achieving satisfactory properties in these nanostructured films [99, 105, 106].

Zavaliche *et al* showed $\Delta E/\Delta H = 100 \text{ V cm}^{-1} \text{ Oe}^{-1}$ at room temperature in a system comprised of CFO pillars embedded in a BFO matrix [107]. These films were analyzed with scanning probe techniques that utilized both magnetized and conducting scanning tips. Typical surface morphology is shown in figure 6(c). Magnetic measurements, show the preference of such structures to maintain magnetization along the length of the nanopillars. Magnetic force microscopy scans both before (figure 6(d)) and after electric poling (figure 6(e)) show a significant number of CFO pillars switch their magnetic state from a downward direction to an upward direction upon application of an electric field [108]. This work further showed that the magnetization-switching event was non-deterministic and could be improved by applying a small magnetic field (700 Oe) to the sample. This field is essential to break time reversal symmetry and overcome the degeneracy between the up and

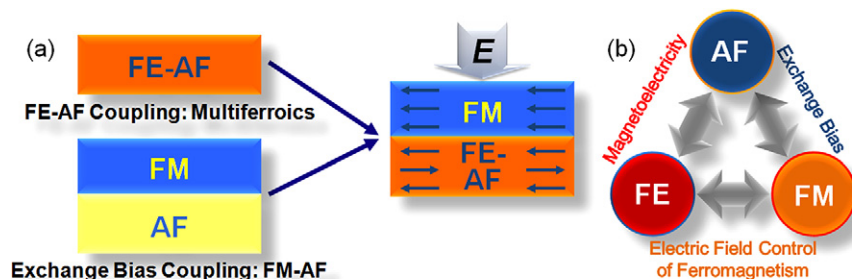


Figure 7. Schematics illustrating the design algorithm for gaining electrical control of ferromagnetism. (a) By combining multiferroics together with traditional ferromagnets, we can create heterostructures that might have new functionalities. (b) These structures rely on two types of coupling—magnetoelectric and exchange bias—to gain electrical control of ferromagnetism by ferroelectric (FE), antiferromagnetic (AF), and ferromagnetic (FM) order.

down magnetization states. Nonetheless, these structures have been shown to be very versatile and offer an excellent opportunity for electrically controlled magnetic storage.

We also note that other interesting nano-scale composite geometries have been investigated. Using anodized aluminum oxide templates, Liu *et al* successfully synthesized nanowires of NiFe_2O_4 surrounded by a shell of PZT [109]. However, successful magnetoelectric coupling has not been yet shown in such a system. Overall, it has been found that nanostructured composite multiferroics have shown significantly enhanced magnetoelectric properties over traditional multilayer heterostructures and are excellent candidates for a wide range of devices that would take advantage of the strong magnetoelectric coupling that can be achieved in these structures.

5. New functionality with multiferroics

One of the major questions in the study of multiferroics today is this: how and when will multiferroics make their way into a room temperature device and what will these devices look like? In early 2005, a number of what were referred to as *magnetoelectronics* based on magnetoelectric materials were proposed [110]. The idea was a simple one, to use the net magnetic moment created by an electric field in a magnetoelectric thin film to change the magnetization of a neighboring FM layer through exchange coupling. The authors went on to propose a number of electrically tunable giant magnetoresistance (GMR) spin valves and tunnel magnetoresistance elements that could be made possible if such structures could be achieved. One additional field that could be greatly affected by this research is the burgeoning field of spintronics. Spin based electronics, or spintronics, have already found successful application in magnetic read-heads and sensors that take advantage of GMR and tunnel magnetoresistance (TMR) effects. The future of spintronics is partially focused on evolving beyond passive magnetoelectronic components, like those used today, to devices which combine memory and logic functions in one [111]. One idea is to combine GMR and TMR device architectures with magnetoelectric materials, such as BFO, where an electric field can be used to control the magnetic configuration of the spintronic device.

So, can we control ferromagnetism at room temperature? One possible solution to this question is to utilize heterostructures of existing multiferroic materials, such as BFO, to create new pathways to functionalities not presented in nature. Such a concept is illustrated in figure 7. The idea is to take advantage of two different types of coupling in materials—*intrinsic* magnetoelectric coupling like that in multiferroic materials such as BFO which will allow for electrical control of antiferromagnetism and the *extrinsic* exchange coupling between ferromagnetic and antiferromagnetic materials—to create new functionalities in materials (figure 7(a)). By utilizing these different types of coupling we can then effectively couple ferroelectric order to ferromagnetic order at room temperature and create an alternative pathway to electrical control of ferromagnetism (figure 7(b)). But what exactly are the opportunities for using a material like BFO to gain electrical control over interactions like exchange bias anisotropy? Until recently the materials and the understanding of these appropriate materials did not exist to make this a plausible undertaking. In the time since the proposal of these magnetoelectronics, studies done on a number of multiferroic materials including YMO [112, 113] and BFO [114–116] show that exchange bias with such systems can be demonstrated in a static manner. Additionally, Borisov *et al* reported that they could affect changes on the exchange bias field in $\text{Cr}_2\text{O}_3(111)/(\text{Co}/\text{Pt})_3$ heterostructures by using a magnetoelectric substrate and a series of different cooling treatments with applied electric and magnetic fields [117]. Dynamic switching of the exchange bias field with an applied electric field, however, remained elusive until a recent report by Laukhin, *et al* focusing on YMO at very low temperatures [118].

Recently significant advancements in the understanding of the interactions present in such heterostructures have been presented. Initial reports noted an inverse relationship between domain size in BFO film and the exchange bias measured in CoFeB/BFO heterostructures [119], but further studies have found a correlation not only to the density of domain walls, but to the density of certain types of domain walls [120]. This same report has identified the importance of 109° domain walls in creating exchange bias and has presented the idea that two distinctly different types of exchange interactions are occurring in heterostructures of $\text{Co}_{0.9}\text{Fe}_{0.1}$ (CoFe)/BFO. The first interaction has been called an *exchange bias* interaction

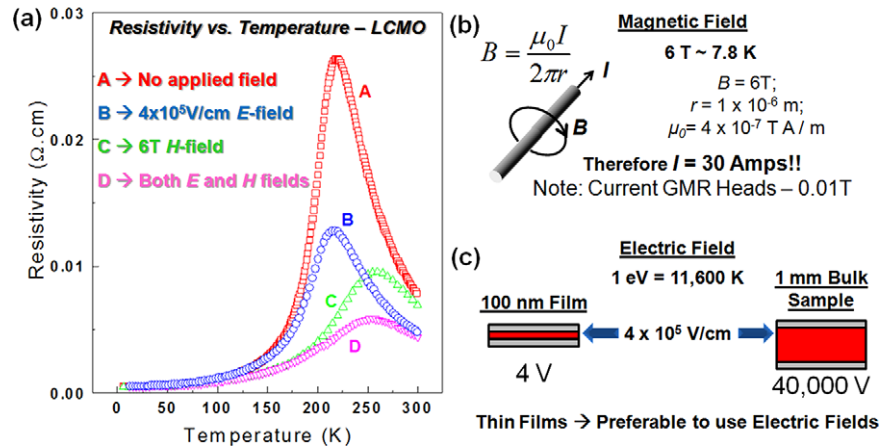


Figure 8. (a) Resistivity versus temperature for $\text{La}_{0.7}\text{Ca}_{0.3}\text{MnO}_3$ thin films with no applied field (red), applied electric field (blue), applied magnetic field (green), and both applied electric and magnetic fields (pink). Energy scales in materials dictate the eventual incorporation of such materials into device structures. (b) The production of the large magnetic fields (~ 6 T) required for colossal magnetoresistance in CMR materials requires large currents (~ 30 A) while (c) production of the appropriate electric fields to produce colossal electroresistance (~ 4 V for a 100 nm thick thin film) are much more reasonable and possible in standard semiconductor electronics circuitry. Adapted from [122].

and takes place between pinned, uncompensated spin occurring at 109° domain walls in BFO and spins in the CoFe layer. This interaction results in a shift of the CoFe hysteresis loop. The second interaction has been called an *exchange enhancement* interaction that arises from an interaction of the spins in the ferromagnet and the fully compensated (001) surface of the G-type antiferromagnetic surface of BFO. This interaction results in an enhancement of the coercive field of the ferromagnetic layer. Utilizing these findings, researchers have moved to create the first room temperature device aimed at gaining electrical control of ferromagnetism with an electric field. Initial results point to the ability to utilize the above *exchange enhancement* interaction to deterministically change the direction of ferromagnetic domains by 90° upon application of an applied electric field [121]. This represents the first example of a room temperature device structure to utilize a multiferroic material to access new functionalities in materials.

6. Future directions and conclusions

We hope that this review has captured some of the exciting new developments in the field of multiferroics and magnetoelectrics, especially from a thin film perspective. New developments are occurring at a rapid pace, throwing further light onto the intricacies of these materials. The dramatic progress in thin film heterostructure and nanostructure growth has been a key enabler fueling these discoveries. Materials discoveries aside, a critical materials physics question emerges from all of the progress, not only in the field of multiferroics but in all of correlated oxides as well. This has to do with the role of energy scales (as well as time and length scales) of relevance to the ultimate implementation of these materials into actual devices. Let us explore this issue a bit more in detail, using the data presented in figure 8 for the colossal magnetoresistant (CMR) manganites (data shown here is for $\text{La}_{0.7}\text{Ca}_{0.3}\text{MnO}_3$ (LCMO)) as a frame of reference. Over the past 15 years, there has been extensive research conducted on these materials. By far the most interesting aspect is the

large change in resistance (colossal) with the application of a magnetic field of several Tesla (6 T in the present example) (shown in the green data in figure 8(a)). It has also been demonstrated that a commensurate ‘colossal electroresistance’ can be obtained with electric fields of the order of a few hundred kV (shown in blue in figure 11(a)) [122]. Let us now compare these two energy scales and ask the question: how do these two types of fields compare from the perspective of external power requirements?

We can understand this through a simple thought experiment. If one needed to generate the necessary magnetic field of 6 T at a distance of $1 \mu\text{m}$ from a metal wire (figure 8(b)), a current of ~ 30 Amps would be required! We note that a 6 T magnetic field translates to a temperature scale in the material of ~ 8 K [123], which is significantly smaller than the critical temperatures (for example the magnetic transition temperature or the peak in the resistivity). Regardless, this current is prohibitive both from the point of view of the integrity of the metal wire that would carry the current as well as the power requirements. Let us now examine the electric field (figure 8(c)). If one desires to create the appropriate electric field needed to observe colossal electroresistance in a 100 nm thick film, a potential of only 4 V is required. This is easily generated by standard semiconductor electronics circuitry. However, if the thickness of the material is, say 1 mm, then a potential of 40 000 V is required to generate the same field.

These two scenarios present two important conclusions. First, if the energy scales for manipulation of these materials (be they CMR or multiferroics) do not become significantly smaller, then the use of magnetic fields to probe and manipulate them becomes technologically prohibitive. Indeed, this can be identified as the most important reason why CMR based systems have not become commercially viable. Second, if these energy scales are indeed maintained, it is clear that using thin film heterostructures and manipulating them with electric fields is a more attractive way to proceed in terms of technological manifestations of these phenomena.

Additionally, one of the biggest challenges facing the field of multiferroics today is the need for room temperature functionality. Despite a concerted effort by a wide number of researchers, the search for intrinsic multiferroics that are simultaneously both magnetic and ferroelectric at room temperature remains a difficult one. Inherent to this the fact that one of the two order parameters, either electronic or magnetic, is often a weak property resulting from either a complicated phase transformation, orbital ordering, geometric frustration, etc in materials. Such order parameters are typically very small in magnitude and occur only in the low temperature phase. Thus, it is essential that the field works to include both thin film heterostructure and bulk synthesis methods and broadens its search for new candidate multiferroics. The interplay between *ab initio*, density functional theoretical approaches and controlled synthetic approaches (be it single crystal growth or MBE-like heteroepitaxial thin film growth) is critical. Thin film heterostructures, further provide an additional degree of freedom through the mismatch strain; here again, the intimate interplay between theoretical predictions [124] and film growth is imperative. Additionally, the authors believe that the field can make significant strides towards room temperature functionality if additional attention is given to utilizing the current materials and technologies widely used in the field today. The work of Chu *et al* [121] represents one pathway to creating new functionalities based on intrinsic multiferroics at room temperature and could be a guide to device designers looking to utilize CMOS compatible control of ferromagnetism in room temperature devices. Finally, it is essential that the field outline the needs and directions of research in the near future. If magnetoelectric coupling is the most interesting figure of merit, composite multiferroics offer extraordinary coupling at room temperature and above. Regardless, the field remains poised to impact everything from basic science to device design in the near future.

By far the most important area of immediate future research has to be a full understanding of the mechanisms by which the magnetic and dielectric order parameters couple in such materials. If deterministic control and manipulation of ferromagnetism is desired, then interactions across heterointerfaces will become important. Domains, domain walls, and defects will undoubtedly play a critical role in unraveling the coupling phenomena. Further, in such heterostructure based coupling, differences between interactions with classical itinerant ferromagnets and double exchange ferromagnets (such as the manganites) need to be explored in depth as well. In thin films, heteroepitaxial constraints (such as strain, clamping, and possibly surface termination) are going to become important variables. Of course, the most desirable situation would be to discover a truly multiferroic material, one that is ferromagnetic and ferroelectric at room temperature and exhibits coupling between these two order parameters. This is truly a challenge for interdisciplinary condensed matter research.

Acknowledgments

The authors acknowledge the support of the Director, Office of Basic Energy Sciences, Materials Science Division of the

US Department of Energy under Contract No. DE-AC02-05CH11231 and previous contracts, ONR-MURI under Grant No. E21-6RU-G4 and previous contracts, and the Western Institute of Nanoelectronics program.

References

- [1] Ramesh R and Spaldin N A 2007 *Nat. Mater.* **6** 21
- [2] Chu Y-H, Martin L W, Holcomb M B and Ramesh R 2007 *Mater. Today* **10** 16
- [3] Schmid H 1994 *Ferroelectrics* **162** 665
- [4] Fiebig M 2005 *J. Phys. D: Appl. Phys.* **38** R123
- [5] Eerenstein W, Mathur N D and Scott J F 2006 *Nature* **442** 759
- [6] Hill N A 2000 *J. Phys. Chem.* **104** 6694
- [7] Wang J *et al* 2003 *Science* **299** 1719
- [8] Cheong S-W and Mostovoy M 2007 *Nat. Mater.* **6** 13
- [9] Schlom D G, Haeni J H, Lettieri J, Theis C D, Tian W, Jiang J C and Pan X Q 2001 *Mater. Sci. Eng. B* **87** 282
- [10] Fujimura N, Ishida T, Yoshimura T and Ito T 1996 *Appl. Phys. Lett.* **69** 1011
- [11] Yakel H L, Koehler W C, Bertaut E F and Forrat E F 1963 *Acta Crystallogr.* **16** 957
- [12] Bertaut E F, Pauthenet R and Mercier M 1963 *Phys. Lett.* **7** 110
- [13] van Aken B B, Palstra T T, Filipetti M and Spaldin N A 2004 *Nat. Mater.* **3** 164
- [14] Salvador P, Doan T-D, Mercey B and Raveau B 1998 *Chem. Mater.* **10** 2592
- [15] Yoo D C, Lee J Y, Kim I S and Kim Y T 2002 *Thin Solid Films* **416** 62
- [16] Suzuki K, Fu D, Nishizawa K, Miki T and Kato K 2003 *Japan. J. Appl. Phys.* **42** 5692
- [17] Dho J, Leung C W, MacManus-Driscoll J L and Blamire M G 2004 *J. Cryst. Growth* **267** 548
- [18] Posadas A, Yau J-B, Ahn C H, Han J, Gariglio S, Johnston K, Rabe K M and Neaton J B 2005 *Appl. Phys. Lett.* **87** 171915
- [19] Chye Y, Liu T, Li D, Lee K, Lederman D and Myers T H 2006 *Appl. Phys. Lett.* **88** 132903
- [20] Kim K T and Kim C L 2004 *J. Eur. Ceram. Soc.* **24** 2613
- [21] Zhou L, Wang Y P, Liu Z G, Zou W Q and Du Y W 2004 *Phys. Status Solidi a* **201** 497
- [22] Shigemitsu N, Sakata H, Ito D, Yoshimura T, Ashida A and Fujimura N 2004 *Japan. J. Appl. Phys.* **43** 6613
- [23] Kim D, Klingensmith D, Dalton D, Olariu V, Gnadinger F, Rahman M, Mahmud A and Kalkur T S 2004 *Integr. Ferroelectr.* **68** 75
- [24] Ito D, Fujimura N, Yoshimura T and Ito T 2003 *J. Appl. Phys.* **93** 5563
- [25] Fujimura N, Sakata H, Ito D, Yoshimura T, Yokota T and Ito T 2003 *J. Appl. Phys.* **93** 6990
- [26] Choi T and Lee J 2004 *Appl. Phys. Lett.* **84** 5043
- [27] Sundaresan A, Maignan A and Raveau B 1997 *Phys. Rev. B* **56** 5092
- [28] Nugroho A A, Bellido N, Adem U, Néner G, Simon Ch, Tjia M O, Mostovoy M and Palstra T T M 2007 *Phys. Rev. B* **75** 174435
- [29] Bosak A A *et al* 2001 *Thin Solid Films* **400** 149
- [30] Suzuki K, Nishizawa K, Miki T and Kato K 2002 *J. Cryst. Growth* **237–239** 482
- [31] Lee J-H *et al* 2006 *Adv. Mater.* **18** 3125
- [32] Balasubramanian K R, Havelia S, Salvador P A, Zheng H and Mitchell J F 2007 *Appl. Phys. Lett.* **91** 232901
- [33] dos Santos A M, Parashar S, Raju A R, Zhao Y S, Cheetham A K and Rao C N R 2002 *Solid State Commun.* **122** 49

- [34] Azuma M, Seiji N, Belik A, Shintaro I, Takashi S, Kazuhide T, Ikuya Y, Yuichi S and Mikio T 2006 *Trans. Mater. Res. Soc. Japan.* **31** 41
- [35] dos Santos A M, Cheetham A K, Tian W, Pan X, Jia Y, Murphy N J, Lettieri J and Schlom D G 2004 *Appl. Phys. Lett.* **84** 91
- [36] Sharan A, Lettieri J, Jia Y, Tian W, Pan X, Schlom D G and Gopalan V 2004 *Phys. Rev. B* **69** 214109
- [37] Atou T, Chiba H, Ohoyama K, Yamaguichi Y and Syono Y 1999 *J. Solid State Chem.* **145** 639
- [38] Son J Y, Kim B G, Kim C H and Cho J H 2004 *Appl. Phys. Lett.* **84** 4971
- [39] Gajek M, Bibes M, Barthélémy A, Bouzehouane K, Fusil S, Varela M, Fontcuberta J and Fert A 2005 *Phys. Rev. B* **72** 020406(R)
- [40] Gajek M, Bibes M, Fusil S, Bouzehouane K, Fontcuberta J, Barthélémy A and Fert A 2007 *Nat. Mater.* **6** 296
- [41] Yang C H, Lee S H, Koo T Y and Jeong Y H 2007 *Phys. Rev. B* **75** 140104
- [42] Belik A A *et al* 2005 *J. Am. Chem. Soc.* **128** 706
- [43] Baettig P, Seshadri R and Spaldin N A 2007 *J. Am. Chem. Soc.* **129** 9854
- [44] Shishidou T, Mikamo N, Uratani Y, Ishii F and Oguchi T 2004 *J. Phys.: Condens. Matter* **16** S5677
- [45] Royen P and Swars K 1957 *Angew. Chem.* **24** 779
- [46] Kubel F and Schmid H 1990 *Acta Crystallogr. B* **46** 698
- [47] Kiselev S V, Ozerov R P and Zhdanov G S 1963 *Sov. Phys.—Dokl.* **7** 742
- [48] Teague J R, Gerson R and James W J 1963 *Solid State Commun.* **8** 1073
- [49] Michel C, Moreau J M, Achenbach G D, Gerson R and James W J 1969 *Solid State Commun.* **7** 701
- [50] Moreau J M, Michel C, Gerson R and James W J 1971 *J. Phys. Chem. Solids* **32** 1315
- [51] Tabares-Muñoz C, Rivera J P, Bezinge A, Monnier A and Schmid H 1985 *Japan. J. Appl. Phys.* **24** 1051
- [52] Zavaliche F, Yang S Y, Zhao T, Chu Y H, Cruz M P, Eom C B and Ramesh R 2006 *Phase Transit.* **79** 991
- [53] Fischer P, Polomska M, Sosnowska I and Szymanski M 1980 *J. Phys. C: Solid State Phys.* **13** 1931
- [54] Sosnowska I, Peterlin-Neumaier T and Steichele E 1982 *J. Phys. C: Solid State Phys.* **15** 4835
- [55] Dzyaloshinskii I E 1957 *Sov. Phys.—JETP* **5** 1259
- [56] Moriya T 1960 *Phys. Rev.* **120** 91
- [57] Neaton J B, Ederer C, Waghmare U V, Spaldin N A and Rabe K M 2005 *Phys. Rev. B* **71** 014113
- [58] Ederer C and Spaldin N A 2005 *Phys. Rev. B* **71** 060401(R)
- [59] Béa H, Bibes M, Fusil S, Bouzehouane K, Jacquet E, Rode K, Bencok P and Barthélémy A 2006 *Phys. Rev. B* **74** 020101
- [60] Gao F, Chen X, Yin K, Dong S, Ren Z, Yuan F, Yu T, Zou Z and Liu J M 2007 *Adv. Mater.* **19** 2889
- [61] Zhao T *et al* 2006 *Nat. Mater.* **5** 823
- [62] Lebeugle D, Colson D, Forget A, Viret M, Bataille A M and Gukasov A 2008 *Preprint* 0802.2915 [cond-mat]
- [63] Palkar V R, John J and Pinto R 2002 *Appl. Phys. Lett.* **80** 1628
- [64] Lee Y H, Lee C C, Liu Z X, Liang C S and Wu J M 2005 *Electrochem. Solid-State Lett.* **8** F55
- [65] Das R R, Kim D M, Baek S H, Zavaliche F, Yang S Y, Ke X, Streiffer S K, Rzechowski M S, Ramesh R and Eom C B 2006 *Appl. Phys. Lett.* **88** 242904
- [66] Yang S Y, Zavaliche F, Mohaddes-Ardabili L, Vaithyanathan V, Schlom D G, Lee Y J, Chu Y H, Cruz M P, Zhao T and Ramesh R 2005 *Appl. Phys. Lett.* **87** 102903
- [67] Ueno R, Okaura S, Funakubo H and Saito K 2005 *Japan. J. Appl. Phys.* **44** L1231
- [68] Singh S K, Kim Y K, Funakubo H and Ishiwara H 2006 *Appl. Phys. Lett.* **88** 062502
- [69] Wang J, Zheng H, Ma Z, Prasertchoung S, Wuttig M, Droopad R, Yu J, Eisenbeiser K and Ramesh R 2004 *Appl. Phys. Lett.* **85** 2574
- [70] Tian W, Vaithyanathan V, Schlom D G, Zhan Q, Yang S Y, Chu Y H and Ramesh R 2007 *Appl. Phys. Lett.* **90** 172908
- [71] Chu Y H *et al* 2007 *Appl. Phys. Lett.* **90** 252906
- [72] Li Y *et al* 2005 *J. Appl. Phys.* **97** 034112
- [73] Chu Y H *et al* 2006 *Adv. Mater.* **18** 2307
- [74] Pabst G W, Martin L W, Chu Y H and Ramesh R 2007 *Appl. Phys. Lett.* **90** 072902
- [75] Chu Y H, Cruz M P, Yang C H, Martin L W, Yang P L, Zhang J X, Lee K, Yu P, Chen L Q and Ramesh R 2007 *Adv. Mater.* **19** 2662
- [76] Lee Y-H, Wu J-M and Lai C-H 2006 *Appl. Phys. Lett.* **88** 042903
- [77] Qi X, Dho J, Tomov R, Blamire M G and MacManus-Driscoll J L 2005 *Appl. Phys. Lett.* **86** 062903
- [78] Kim J K, Kim S S, Kim W-J, Bhalla A S and Guo R 2006 *Appl. Phys. Lett.* **88** 132901
- [79] Murakami M, Fujino S, Lim S-H, Long C J, Salamanca-Rib L G, Wuttig M, Takeuchi I, Nagarajan V and Varatharajan A 2006 *Appl. Phys. Lett.* **88** 152902
- [80] Belik A A *et al* 2006 *Chem. Mater.* **18** 798
- [81] Urantani Y, Shishidou T, Ishii F and Oguchi T 2005 *Japan. J. Appl. Phys.* **44** 7130
- [82] Yasui S, Nishida K, Naganuma H, Okamura S, Iijima T and Funakubo H 2007 *Japan. J. Appl. Phys.* **46** 6948
- [83] Martin L W, Zhan Q, Suzuki Y, Ramesh R, Chi M, Browning N, Mizoguchi T and Kreisel J 2007 *Appl. Phys. Lett.* **90** 062903
- [84] Kumar A, Martin L W, Denev S, Kortright J B, Suzuki Y, Ramesh R and Gopalan V 2007 *Phys. Rev. B* **75** 060101(R)
- [85] Sakai M, Msauno A, Kan D, Hashisaka M, Takata K, Azume M, Takano M and Shimakawa Y 2007 *Appl. Phys. Lett.* **90** 072903
- [86] Van den Boomgaard J, Terrell D R and Born R A J 1974 *J. Mater. Sci.* **9** 1705
- [87] Avellaneda M and Harshe G 1994 *J. Intell. Mater. Syst. Struct.* **5** 501
- [88] Ryu J, Priya S, Carazo A V, Uchino K and Kim H 2001 *J. Am. Ceram. Soc.* **84** 2905
- [89] Ryu S, Park J H and Jang H M 2007 *Appl. Phys. Lett.* **91** 142910
- [90] Ryu J, Carazo A V, Uchino K and Kim H 2001 *J. Electroceram.* **7** 17
- [91] Srinivasan G, Rasmussen E T, Gallegos J and Srinivasan R 2001 *Phys. Rev. B* **64** 214408
- [92] Srinivasan G, Rasmussen E T, Levin B J and Hayes R 2002 *Phys. Rev. B* **65** 134402
- [93] Srinivasan G, Rasmussen E T, Bush A A and Kamentsev K E 2004 *Appl. Phys. A* **78** 721
- [94] Ryu J, Priya S, Uchino K and Kim H E 2002 *J. Electroceram.* **8** 107
- [95] Murugavel P, Singh M P, Prellier W, Mercey B, Simon C and Raveau B 2005 *J. Appl. Phys.* **97** 103914
- [96] Stein S, Wuttig M, Viehland D and Quandt E 2005 *J. Appl. Phys.* **97** 10Q301
- [97] Bichurin M I, Petrov V M and Srinivasan G 2003 *Phys. Rev. B* **68** 054402
- [98] Zheng H *et al* 2004 *Science* **303** 661
- [99] Zheng H, Zhan Q, Zavaliche F, Sherburne M, Straub F, Cruz M P, Chen L-Q, Dahmen U and Ramesh R 2006 *Nano Lett.* **7** 1401
- [100] Li J, Levin I, Slutsker J, Provenzano V, Schenck P K, Ramesh R, Ouyang J and Roytburd A L 2005 *Appl. Phys. Lett.* **87** 072909
- [101] Wan J G, Wang X W, Wu Y J, Zeng M, Wang Y, Jiang H, Zhou W Q, Wang G H and Liu J M 2005 *Appl. Phys. Lett.* **86** 122501

- [102] Ren S and Wuttig M 2007 *Appl. Phys. Lett.* **91** 083501
- [103] Zhan Q, Yu R, Crane S P, Zheng H, Kisielowski C and Ramesh R 2006 *Appl. Phys. Lett.* **89** 172902
- [104] Murakami M, Fujino S, Lim S-H, Salamanca-Riba L G, Wuttig M, Takeuchi I, Varughese B, Sugaya H, Hasegawa T and Lofland S E 2006 *Appl. Phys. Lett.* **88** 112505
- [105] Ryu H *et al* 2006 *Appl. Phys. Lett.* **89** 102907
- [106] Wan J-G, Weng Y, Wu Y, Li Z, Liu J-M and Wang G 2007 *Nanotechnology* **18** 465708
- [107] Zavaliche F *et al* 2005 *Nano Lett.* **5** 1793
- [108] Zavaliche F, Zhao T, Zheng H, Straub F, Cruz M P, Yang P-L, Hao D and Ramesh R 2007 *Nano Lett.* **7** 1586
- [109] Liu M, Li X, Imrane H, Chen Y, Goodrich T, Cai Z, Ziemer K S and Huang J Y 2007 *Appl. Phys. Lett.* **90** 152501
- [110] Binek Ch and Doudin B 2005 *J. Phys.: Condens. Matter* **17** L39
- [111] Ney A, Pampuch C, Koch R and Ploog K H 2003 *Nature* **425** 485
- [112] Dho J and Blamire M G 2005 *Appl. Phys. Lett.* **87** 252504
- [113] Martí X, Sánchez F, Fontcuberta J, García-Cuenca M V, Ferrater C and Varela M 2006 *J. Appl. Phys.* **99** 08P302
- [114] Dho J, Qi X, Kim H, MacManus-Driscoll J L and Blamire M G 2006 *Adv. Mater.* **18** 1445
- [115] Béa H, Bibes M and Cherifi S 2006 *Appl. Phys. Lett.* **89** 242114
- [116] Martin L W, Chu Y H, Zhan Q, Ramesh R, Han S J, Wang S X, Warusawithana M and Schlom D G 2007 *Appl. Phys. Lett.* **91** 172513
- [117] Borisov P, Hochstrat A, Chen X, Kleeman W and Binek C 2005 *Phys. Rev. Lett.* **94** 117203
- [118] Laukhin V, Skumryev V, Martí X, Hrabovsky D, Sánchez F, García-Cuenca M V, Ferrater C, Varela M, Lüunders U and Fontcuberta J 2006 *Phys. Rev. Lett.* **97** 227201
- [119] Béa H, Bibes M, Ott F, Dupé B, Zhu X H, Petit S, Fusil S, Deranlot C, Bousehouane K and Barthélémy A 2008 *Phys. Rev. Lett.* **100** 017204
- [120] Martin L W, Chu Y H, Holcomb M B, Huijben M, Han S J, Lee D, Wang S X and Ramesh R 2008 *Nano Lett.* **8** 2050
- [121] Chu Y H, Martin L W, Holcomb M B, Gajek M, Han S J, He Q, Balke N, Yang C H, Lee D, Hu W, Zhan Q, Yang P L, Fraile-Rodriguez A, Scholl A and Ramesh R 2008 *Nat. Mater.* **7** 478–82
- [122] Wu T, Ogale S B, Garrison J E, Nagaraj B, Biswas A, Chen Z, Greene R L, Ramesh R and Venkatesan T 2001 *Phys. Rev. Lett.* **86** 5998
- [123] Dagotto E 2003 *Nanoscale Phase Separation and Colossal Magnetoresistance* (New York: Springer)
- [124] Fennie C J and Rabe K M 2007 *Phys. Rev. Lett.* **97** 267602